Translational Oncology
www.transonc.com

Volume 9 Number 4 August 2016 pp. 263–273 263

Targeting Focal Adhesion Kinase Suppresses the Malignant Phenotype in Rhabdomyosarcoma Cells[1]

Alicia M. Waters*, Laura L. Stafman*, Evan F. Garner*, Smitha Mruthyunjayappa*, Jerry E. Stewart*, Elizabeth Mroczek-Musulman† and Elizabeth A. Beierle*

*Department of Surgery, Division of Pediatric Surgery, University of Alabama, Birmingham, AL; †Department of Pathology, University of Alabama, Birmingham, AL

Abstract

Despite the tremendous advances in the treatment of childhood solid tumors, rhabdomyosarcoma (RMS) continues to provide a therapeutic challenge. Children with metastatic or relapsed disease have a disease-free survival rate under 30%. Focal adhesion kinase (FAK) is a nonreceptor tyrosine kinase that is important in many facets of tumorigenesis. Signaling pathways both upstream and downstream to FAK have been found to be important in sarcoma tumorigenesis, leading us to hypothesize that FAK would be present in RMS and would impact cellular survival. In the current study, we showed that FAK was present and phosphorylated in pediatric alveolar and embryonal RMS tumor specimens and cell lines. We also examined the effects of FAK inhibition upon two RMS cell lines utilizing parallel approaches including RNAi and small molecule inhibitors. FAK inhibition resulted in decreased cellular survival, invasion, and migration and increased apoptosis. Furthermore, small molecule inhibition of FAK led to decreased tumor growth in a nude mouse RMS xenograft model. The findings from this study will help to further our understanding of the regulation of tumorigenesis in RMS and may provide desperately needed novel therapeutic strategies for these difficult-to-treat tumors.

Translational Oncology (2016) 9, 263–273

Introduction

Rhabdomyosarcoma (RMS) is a mesodermal cancer that undergoes partial skeletal muscle differentiation. RMS is the fourth most common solid tumor in children, with two thirds of the patients being less than 10 years of age at diagnosis [1]. These tumors are not restricted to children, and it is estimated that over 40% of all RMSs are actually diagnosed in adults [2]. RMS was long considered to have two main subtypes: alveolar and embryonal. Traditionally, the alveolar subtype was considered the more aggressive tumor with poorer outcomes. Current data have shown that it is actually the presence of a *PAX-FOXO1* gene fusion that portends the worse prognosis [3]. Overall survival for RMS has not improved significantly since the 1990s, and survival is currently less than 30% for children with metastatic disease [4]. Survival for adults is equally dismal; over 70% of those diagnosed with RMS will expire from their disease [2]. Novel, less toxic, and innovative therapies are clearly needed.

Focal adhesion kinase (FAK) is a nonreceptor tyrosine kinase that localizes to focal adhesions and controls a number of cellular pathways involved in cell adhesion, migration, invasion, proliferation, and survival [5–8]. FAK activation occurs when cell surface integrins bind to β subunits of FAK, resulting in phosphorylation and binding of Src family kinases [5]. FAK also has an autophosphorylation site at the tyrosine 397 (Y397) residue [9] that leads to increased cell survival via inhibition of detachment-activated apoptosis, or anoikis [10]. FAK inhibition with small interfering RNA (siRNA) [11,12] has been

Address all correspondence to: Elizabeth A. Beierle, 1600 7th Avenue South, Lowder Room 300, Birmingham, AL, 35233.
E-mail: elizabeth.beierle@childrensal.org
[1] The work presented was funded in part by a grant from the National Cancer Institute (T32CA091078) (A.M.W., L.L.S., and E.F.G.).
Received 30 March 2016; Revised 4 June 2016; Accepted 6 June 2016

1936-5233/16
http://dx.doi.org/10.1016/j.tranon.2016.06.001

shown to decrease tumor cell survival. Additionally, abrogation of FAK phosphorylation at Y397 using dominant negative constructs [13] and small molecule inhibitors [12,14–16] has been shown to decrease tumor cellular migration, invasion, and survival.

A previous study with a fibrosarcoma cell line showed that FAK activation occurred in response to a pressure stimulus [17]. This finding led us to hypothesize that RMS would express FAK and that inhibition of FAK would result in a less aggressive phenotype. We demonstrated that abrogation of FAK in both alveolar (*PAX-FOXO1* gene fusion positive) [18] and embryonal (*PAX-FOXO1* gene fusion negative) RMS tumor cell lines resulted in decreased tumor cell survival *in vitro* and decreased xenograft growth *in vivo*. From these studies, we concluded that targeting FAK may prove to be a useful therapeutic adjunct in the treatment of these aggressive solid tumors.

Materials and Methods

Cells and Cell Culture

All cell lines were maintained in standard culture conditions at 37°C and 5% CO_2. RD human embryonal RMS cells (CCL-136; American Type Culture Collection, ATCC, Manassas, VA) were maintained in Dulbecco's modified Eagle's medium containing 10% fetal bovine serum (S11150; Atlanta Biologicals, Flowery Branch, GA), 4 mM L-glutamine, 1 μM nonessential amino acids, and 1 μg/ml penicillin/streptomycin. SJCRH30 human alveolar RMS cells (*PAX-FOXO1* fusion positive) [18] (CRL-2061, ATCC) were maintained in RPMI 1640 medium supplemented with 10% fetal bovine serum (Atlanta Bioligcals) and 1 μg/ml penicillin/streptomycin. All cell lines were obtained from ATCC within the last 2 years and were mycoplasma free.

Antibodies and Reagents

Monoclonal mouse anti-FAK (4.47, 05-0537) antibody was from Millipore (EMD Millipore, Billerica, MA), and rabbit polyclonal anti-phospho-FAK (Y397, 71-7900) antibody was from Invitrogen (Invitrogen Corp., Carlsbad, CA). Rabbit polyclonal anti-cleaved PARP (9542) and rabbit monoclonal anti-PARP (9532) antibodies were obtained from Cell Signaling Technology (Danvers, MA). Monoclonal mouse anti-β-actin was from Sigma (A1978; Sigma-Aldrich Corp., St. Louis, MO). The small molecule PF-573,228 ($C_{22}H_{20}F_3N_5O_3S$) was purchased from Santa Cruz Biotechnology (Santa Cruz, CA), and the small molecule 1,2,4,5-benzenetetraamine tetrahydrochloride (Y15) ($C_6H_{10}N_4 \cdot 4ClH$) from Sigma.

Human Tissue Specimens

Formalin-fixed, paraffin-embedded pediatric RMS tumor specimens were obtained from the tumor repository at our institution under waiver of informed consent from the University of Alabama, Birmingham, institutional review board approval (X1009300009).

Immunohistochemistry Human Specimens

Formalin-fixed, paraffin-embedded human tumor specimens were sectioned into 6-μM sections and baked at 70°C for 1 hour on positive slides. Slides were deparaffinized, steamed, sections quenched with 3% hydrogen peroxide and blocked with blocking buffer (BSA, powdered milk, Triton X-100, PBS) for 30 minutes at 4°C. The primary antibodies anti-FAK (4.47), 1:500 (05-537, Millipore), and anti-phospho-FAK (Y397), 1:500 (04-974, Millipore), were added and incubated overnight at 4°C. After washing with PBS, the secondary antibodies for mouse (ImmPress MP-7402; Vector Laboratories, Burlingame, CA) and rabbit (Super Picture HRP, 87-9263; Zymed Laboratories, Invitrogen) were added (1:10 dilution) for 1 hour at 22°C. The staining reaction was developed with VECTASTAIN Elite ABC kit (PK-6100, Vector Laboratories), TSA (biotin tyramide reagent, 1:400; PerkinElmer, Inc., Waltham, MA), and DAB (Metal Enhanced DAB Substrate, Thermo Fisher Scientific). Slides were counterstained with hematoxylin. Negative controls [mouse IgG (1 μg/ml, Invitrogen) or rabbit IgG (1 μg/ml, EMD Millipore)] were included with each run.

Immunohistochemical Scoring

Stained slides of human tumors were reviewed and scored by two pathologists (S.M., E.M.M.) blinded to the patients. Specimens were scored based upon the intensity of staining and the percentage of tumor cells staining positive and assigned a score from 0 to 3. Scores ranged from negative (no staining) to weak (1), moderate (2), and strong (3).

Immunoblotting

Western blots were performed as previously described [16,19]. Briefly, whole cell lysates or homogenized xenograft specimens were isolated using RIPA [10 mM Tris base pH 7.2, 150 mM NaCl, 1% Na-deoxycholate, 1% Triton X-100, 0.1% sodium dodecyl sulfate (SDS)] lysis buffer supplemented with protease inhibitors (Sigma), phosphatase inhibitors (Sigma), and phenylmethanesulfonylfluoride. Lysates were cleared by centrifugation at 14,000 rpm for 30 minutes at 4°C. Protein concentrations were determined using Bio-Rad kit (Bio-Rad, Hercules, CA) and separated by electrophoresis on sodium dodecyl sulfate polyacrylamide (SDS-PAGE) gels. Antibodies were used according to manufacturer's recommended conditions. Molecular weight markers (Bio-Rad) confirmed the expected size of the target proteins. Immunoblots were developed with Luminata Classico or Crescendo ECL (EMD Millipore). Blots were stripped with stripping solution (Bio-Rad) at 37°C for 15 minutes and then reprobed with selected antibodies. Equal protein loading was confirmed with immunoblotting with antibody to β-actin.

siRNA Transfection

siRNAs were obtained from Dharmacon (Dharmacon, GE Healthcare, Layfayette, CO) for the following FAK target sequences: FAK2, 5′-GGGCAUCAUUCAGAAGAUA-3′; FAK3, 5′-UAGUACAGCUCUUGCAUAU-3′; FAK4 5′-GGACAUUAUUGGCCACUGU-3′. Cells (3×10^5 cells per well) were treated with HiPerFect (Qiagen, Valencia, CA) alone; HiPerFect plus 20 nM negative control siRNA (1027310, Qiagen); or HiPerFect plus FAK siRNA2, 3, or 4 (20 nM) according to manufacturer's protocol, incubated for 24 to 48 hours following transfection, and then used for experiments. FAK inhibition by siRNA was confirmed using immunoblotting.

Cell Viability Assays

Cell viability was measured with alamarBlue assay. Briefly, 1.5×10^3 cells per well were plated on 96-well culture plates; allowed to attach; and treated with RNAi inhibition, PF-573,228 (PF, Santa Cruz), or 1,2,4,5-benzenetetraamine tetrahydrochloride (Y15, Sigma). Following treatment, 10 μl of alamarBlue dye (Invitrogen) was added and after 4 to 6 hours; the absorbance at 595 nm was measured using a kinetic microplate reader (BioTek Gen5; BioTek Instruments, Winooski, VT). Viability was reported as fold change.

Proliferation

Proliferation was measured with CellTiter 96 assay according to manufacturer's recommendations (CellTiter 96 AQueous One

Solution Cell Proliferation Assay; Promega, Madison, WI). Briefly, RD or SJCRH30 cells (5×10^3 cells per well) were treated with HiPerFect (Qiagen) alone; control negative siRNA (siNeg, Qiagen); or siFAK2, 3, or 4 (Dharmacon) for 48 hours. Cells were stained with 10 μl of CellTiter 96 dye, and the absorbance at 490 nm was measured using a kinetic microplate reader (BioTek Gen5). For experiments with PF (Santa Cruz) and Y15 (Sigma), similar cell numbers were plated, and cells were treated for 48 hours with increasing concentrations of PF or Y15. Proliferation was evaluated with CellTiter 96 and reported as fold change.

Migration Assay

Twelve-well culture plates (TransWell; Corning Inc., Lowell, MA) with 8-μm micropore inserts were used. The bottom side of the insert was coated with collagen type I (10 mg/ml, 50 μl for 4 hours at 37°C). RD or SJCRH30 cells were treated with PF-573,228 or Y15 and placed into the upper well at a concentration of 5×10^3 cells per well and allowed to migrate for 24 hours. The inserts were then fixed with 3% paraformaldehyde and stained with crystal violet, and migrated cells were counted with a light microscope. Migration was reported as fold change.

Invasion Assay

Similar to migration, 12-well culture plates (TransWell, Corning) with 8-μm micropore inserts were used. The top side of the insert was coated with Matrigel (BD Biosciences, San Jose, CA) (1 mg/ml, 50 μl for 4 hours at 37°C). RD or SJCRH30 cells (5×10^3 cells per well) were treated with PF-573,228 or Y15 and plated into the upper well. Cells were allowed to invade for 48 hours. The inserts were then fixed with 3% paraformaldehyde and stained with crystal violet, and cells were counted with a light microscope. Invasion was reported as fold change.

In Vivo Tumor Growth

All experiments were performed in strict accordance with the recommendations in the *Guide for the Care and Use of Laboratory Animals* of the National Institutes of Health. The protocol was approved by the University of Alabama, Birmingham, Institutional Animal Care and Use Committee (120209355) in compliance with institutional, national, and National Institutes of Health animal use guidelines. Six-week-old female athymic nude mice (Harlan Laboratories, Inc., Chicago, IL) were maintained in the SPF animal facility with standard 12-hour light/dark cycles and allowed chow and water *ad libitum*. Human RMS cells, RD (2.5×10^6 cells/100 μl of sterile PBS), were injected into the subcutaneous space of the right flank (n = 25). Tumors were measured every 2 days, and tumor volumes were calculated with the standard formula of $[(\text{width})^2 \times \text{length}]/2$, where width was the shorter length. When tumors reached 200 mm^3, the animals were randomized to receive daily intraperitoneal injections of either control vehicle (saline, 100 μl, n = 10) or 1,2,4,5-benzenetetraamine tetrahydrochloride (Y15, 30 mg/kg per day, 100 μl, n = 15). This dose was chosen based upon prior *in vivo* studies with Y15 [14–16,19]. Y15 treatment continued for 2 weeks, at which time control animals met IACUC parameters for euthanasia and all animals were euthanized with CO_2 and bilateral thoracotomy and the flank tumors harvested. The incidence of tumor occurrence was not different between the treatment groups, and all animals (n = 25) developed tumors. Data were reported as change in tumor volume from initiation of treatment. This same experiment was also completed with the SJCRH30 cell line but with fewer cells injected (2.0×10^6 cells/100 μl of sterile PBS) because of their growth characteristics.

Immunohistochemistry Murine Samples

Formalin-fixed, paraffin-embedded tumor blocks of murine RMS xenografts were cut in 6-μM sections. The slides were baked for 1 hour at 70°C, deparaffinized, rehydrated, and steamed. The sections were then quenched with 3% hydrogen peroxide and blocked with PBS-blocking buffer. Ki67 staining for cellular proliferation in the tumor xenografts was completed. The primary anti-Ki67 rabbit polyclonal antibody (ab15580; Abcam, Cambridge, MA) was added (1:200 dilution) and incubated overnight at 4°C. After washing with PBS, the secondary antibody (donkey anti-rabbit, 1:400; Jackson ImmunoResearch Laboratories, West Grove, PA) was added for 1 hour at 22°C. The staining reactions were developed with VECTASTAIN Elite ABC kit (PK-6100, Vector Laboratories), TSA (1:400, PerkinElmer, Inc.), and DAB (ImmPACT DAB, Vector Laboratories). Slides were counterstained with hematoxylin. A negative control [rabbit IgG (1 μg/ml, EMD Millipore)] was included with each run.

Data Analysis

Data reported as mean ± standard error of the mean. Densitometry of Western blots was performed using the image histogram analysis feature of Adobe Photoshop software (Adobe Systems Inc., San Jose, CA). Ki67 staining was quantified by ImageJ software (http://rsb.info.nih.gov/ij/). Positive Ki67 staining was reported as percent positive staining cells per high-power field after counting 10 random fields of view per specimen. Student's t test, Fisher's exact test, or analysis of variance was used as appropriate to compare data between groups. Statistical significance was determined at the $P < .05$.

Results

FAK in Pediatric RMS Specimens and Cell Lines

To determine if FAK may be clinically relevant, immunohistochemistry was performed on 15 human pediatric RMS tumor specimens, including 6 alveolar and 9 embryonal histologic types. FAK staining was detected in all six of the alveolar and in eight of the nine embryonal specimens. In addition, FAK was phosphorylated in all 14 of the specimens in which it was detected. Representative photomicrographs are presented in Figure 1*A* (20×) (Figure 1*A*, *brown stain*). There were no significant differences noted in the stain scores of either pY397FAK (Figure 1*B*, *bar* = *median*) or FAK between the two subtypes (Figure 1*C*, *bar* = *median*). Immunoblotting was used to evaluate FAK expression in the SJCRH30 and RD RMS tumor cell lines. FAK was detected in both of the cell lines and was phosphorylated (Figure 1*D*).

Decreased RMS Cell Viability and Proliferation with FAK siRNA

We initially studied the effects of FAK silencing with siRNA on RD and SJCRH30 cell viability. RD and SJCRH30 cells were treated with HiPerFect plus negative control siRNA (siNeg, 20 nM) or HiPerFect plus siRNA specific for FAK (siFAK2, 3, or 4; 20 nM) for 48 hours. siRNA treatment of the cell lines successfully inhibited FAK protein expression (Figure 2*A*). Cellular viability was measured using alamarBlue following FAK knockdown with siRNA. In the RD cell line treated with siFAK, cell viability decreased significantly following treatment (1.0 ± 0 vs 0.87 ± 0.0005 and 0.64 ± 0.01, $P \leq .01$, siNeg vs siFAK3 or siFAK4, respectively) (Figure 2*B*). In the SJCRH30 cell line, cell viability was also decreased significantly (1.0 ± 0.03 vs 0.72 ± 0.005 and 0.71 ± 0.002, $P \leq .01$, siNeg vs siFAK2 or

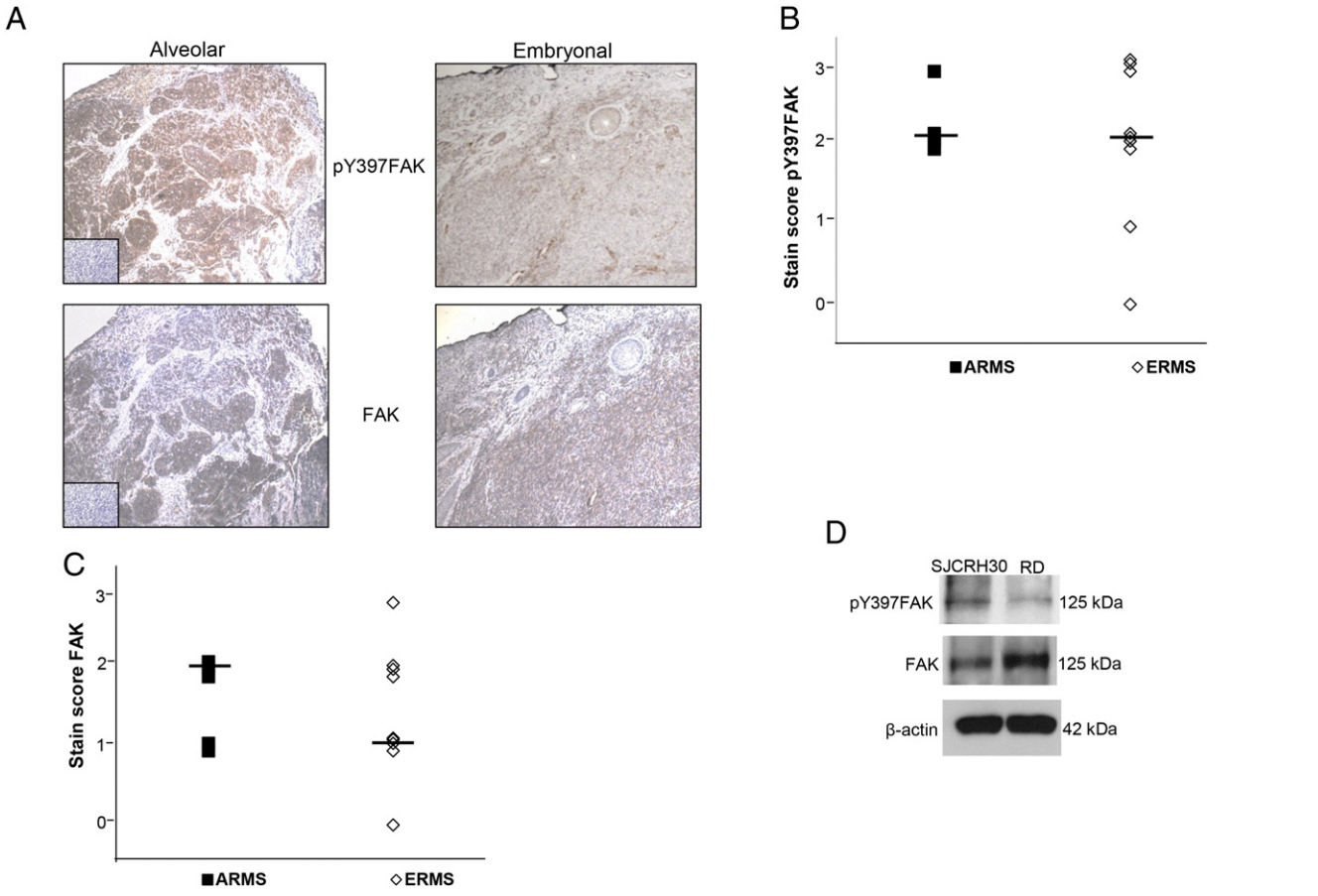

Figure 1. FAK in pediatric RMS specimens and cell lines. (A) Immunohistochemistry staining with antibodies specific for FAK and pY397FAK was performed on 15 formalin-fixed, paraffin-embedded human pediatric RMS tumor specimens (6 alveolar and 9 embryonal). Representative photomicrographs presented at 20× show staining for FAK (lower panels) and pY397 FAK (upper panels) in both histologic types. Negative controls (mouse or rabbit IgG) were included with each run (inserts, bottom left upper and lower panels). (B) Immunohistochemical staining was scored. Stain scores for pY397FAK staining were similar between ARMS and ERMS specimens. Bars represent the mean stain scores. (C) Immunohistochemical staining was scored for FAK staining. Stain scores for FAK were not different between ARMS and ERMS specimens. The bar represents the median stain scores. (D) Immunoblotting for pY397FAK and total FAK was performed on SJCRH30 and RD RMS tumor cell lysates. FAK was detected in both cell lines and was phosphorylated.

siFAK3, respectively) (Figure 2*B*). To determine whether cell proliferation was affected by FAK inhibition, CellTiter 96 was performed following 48-hour treatment with siRNA (20 nM). Both the RD and the SJCRH30 cell lines showed a significant decrease in proliferation following FAK knockdown with siRNA when compared with siNeg (Figure 2*C*).

PF-573,228 Decreased Cell Survival and Motility

To examine the effects of FAK inhibition, we utilized a small molecule FAK inhibitor, PF-573,228 (PF). PF targets the ATP-binding pocket of FAK and has been shown in multiple cell lines to block FAK phosphorylation at the tyrosine 397 (Y397) site [20]. Cells were treated with PF at increasing concentrations. Immunoblotting was utilized to confirm pY397FAK inhibition. After 48 hours of treatment, PF decreased FAK phosphorylation (Y397) in both cell lines (Figure 3*A*). AlamarBlue assays were used to assess the effects of PF on cell survival. Both RD and SJCRH30 cell lines showed significantly decreased cell survival following treatment with PF for 48 hours (Figure 3*B*). The calculated LD_{50} for PF was 28 μM in the RD cell line and 40 μM in the SJCRH30 cell line. To determine whether the PF-induced cell death was due to apoptosis, immunoblotting for cleaved PARP was examined. There was an increase in cleaved PARP expression in both cell lines after treatment with PF (Figure 3*C*), indicating that decreased cell viability was due to apoptosis. Furthermore, cleavage of caspase 3 was measured with a detection kit and confirmed apoptosis in both cell lines following PF treatment (Figure 3*D*). We also examined cell proliferation with CellTiter 96 assays. There was a significant decrease in proliferation in both cell lines following treatment with PF for 48 hours (Supplemental Data Figure S1*A*).

FAK also affects cell migration and invasion [12,21]; therefore, we wished to determine if these entities would be affected by FAK inhibition in RMS cell lines. For invasion, RD and SJCRH30 cell lines were treated with increasing concentrations of PF and allowed to invade through a Matrigel layer. PF significantly inhibited cell invasion in both cell lines (Figure 4*A*). Migration was also evaluated with Transwell assays. There was a significant decrease in cell migration in both cell lines following increasing concentrations of PF (Figure 4*B*). In both invasion and migration, the changes noted were at concentrations of PF that were well below the calculated LD_{50} for the cell lines, indicating that these changes were not simply secondary to cell death.

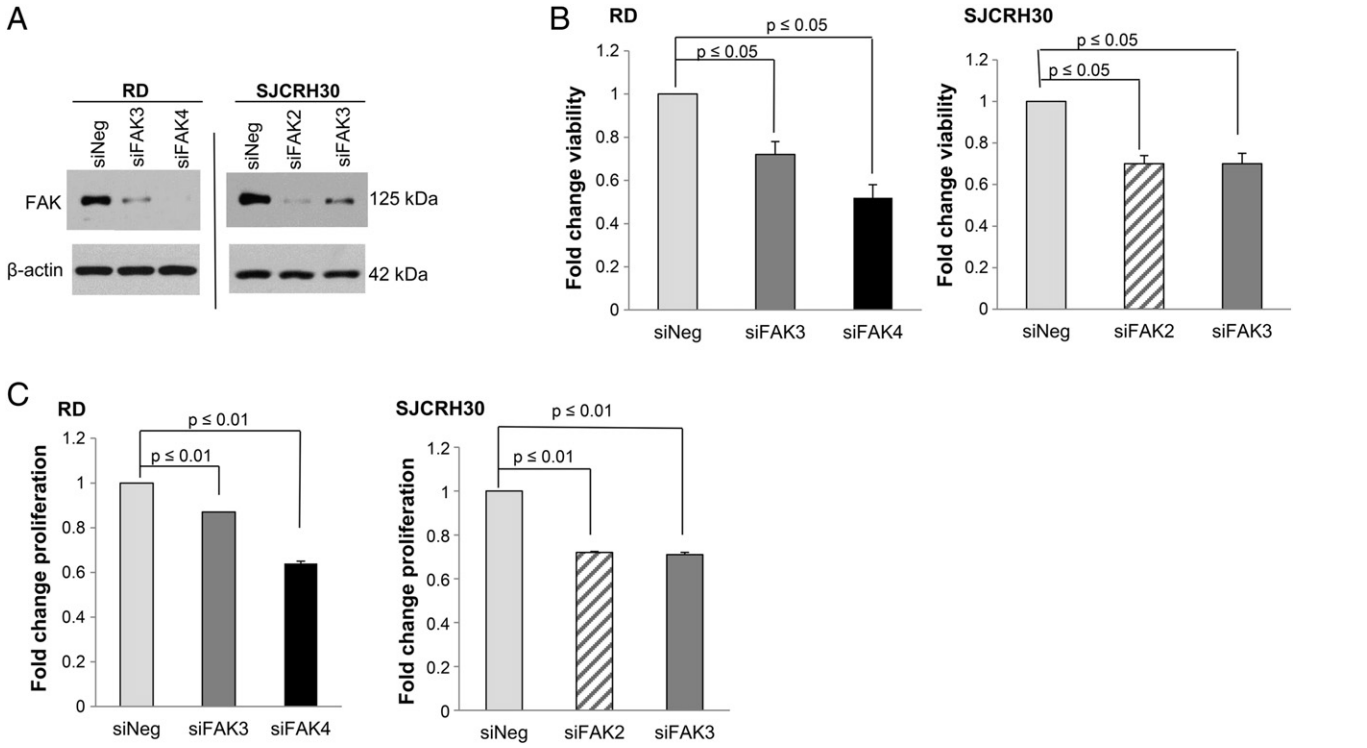

Figure 2. FAK knockdown with siRNA. (A) RD and SJCRH30 cells were treated with negative control siRNA (siNeg) or multiple independent siRNAs specific for FAK (siFAK2, siFAK3, siFAK4, 20 nM) for 48 hours. Immunoblotting for FAK showed decreased FAK expression in both cell lines with siFAK treatment. (B) RD and SJCRH30 cells were treated with siFAK2, 3, or 4 (20 nM) for 48 hours; cellular viability was measured using alamarBlue assay and reported as fold change in viability. In both cell lines, viability decreased significantly following treatment with siFAK knockdown. (C) RD and SJCRH30 cells were treated with siFAK2, 3, or 4 (20 nM) for 48 hours, and cellular proliferation was measured using CellTiter 96. There was a decrease in proliferation in both cell lines that was significant from the cells treated with siNeg. Data were from three independent experiments and reported as mean fold change ± SEM.

1,2,4,5-Benzenetetraamine Tetrahydrochloride (Y15) Decreased Cell Survival, and Motility

PF was not formulated for use *in vivo*[20], and we wished to advance these studies to an animal model. Therefore, we chose to investigate 1,2,4,5-benzenetetraamine tetrahydrochloride (Y15), one of only a few small molecule FAK inhibitors that can be used in animals [15,16]. Y15 has been previously described and was designed to inhibit Y397 phosphorylation of FAK [14] but also inhibits total FAK expression [15,16]. Using immunoblotting, we showed that Y15 decreased FAK expression in both the RD and SJCRH30 cell lines (Figure 5*A*). Next, we examined how Y15 treatment affected cell viability using alamarBlue assays. Both RD and SJCRH30 cell lines showed significantly decreased cell viability following treatment with Y15 (Figure 5*B*). The calculated LD_{50} for Y15 was 23 μM in the RD and 7 μM in the SJCRH30 cell line. Additionally, the cell death caused by Y15 in both cell lines was via apoptosis, as demonstrated by decreased total PARP by immunoblotting (Figure 5*C*). Caspase 3 cleavage was also measured with a detection kit, and in the RD cell line following Y15 treatment, there was cleavage of caspase 3 further demonstrating apoptosis (Figure 5*D*). Cell proliferation was evaluated with CellTiter 96 assays. There was a significant decrease in proliferation in both cell lines following treatment with Y15 for 48 hours (Supplemental Data Figure S1*B*).

Phenotypic changes in the RD and SJCRH30 tumor cell lines following Y15 treatment were further evaluated with cell invasion and migration. RD and SJCRH30 cells were treated with increasing concentrations of Y15. Invasion was measured after 48 hours, and there was a significant decrease in invasion in both cell lines with Y15 (Figure 6*A*). In addition, after 24 hours of Y15, the cell lines showed a marked decrease in migration by Transwell assay (Figure 6*B*). As seen with PF, the phenotypic changes following Y15 occurred at concentrations well below the LD_{50} concentration of Y15 for both cell lines, indicating that these findings were not solely due to cell death.

1,2,4,5-Benzenetetraamine Tetrahydrochloride (Y15) Treatment In Vivo

To test the *in vivo* effects of FAK inhibition, a nude mouse model of RMS was used. RD human ERMS cells (2.5×10^6) were injected into the right flank of 6-week-old female athymic nude mice ($n = 25$). Tumors were measured every 2 days, and tumor volumes were calculated with the standard formula of $[(\text{width})^2 \times \text{length}]/2$, where width is the shorter length. When tumors reached 200 mm^3, animals were randomized to receive intraperitoneal injections with either control (saline, $n = 10$) or Y15 ($n = 15$) for 2 weeks. Data were reported as change in tumor volume from the time treatment began. Animals treated with Y15 had significantly less tumor growth than control-treated animals ($P = .05$) (Figure 7, *A* and *B*). The time for tumor tripling was increased in the Y15-treated tumors compared with vehicle-treated tumors but did not reach statistical significance (5.1 ± 1.8 days vs 6.3 ± 1.3 days, NS, vehicle vs Y15). To demonstrate target knockdown, tumor lysates were examined using immunoblotting for FAK expression. Representative immunoblots are shown in Figure 7*C*. Tumors from Y15-treated animals had less FAK

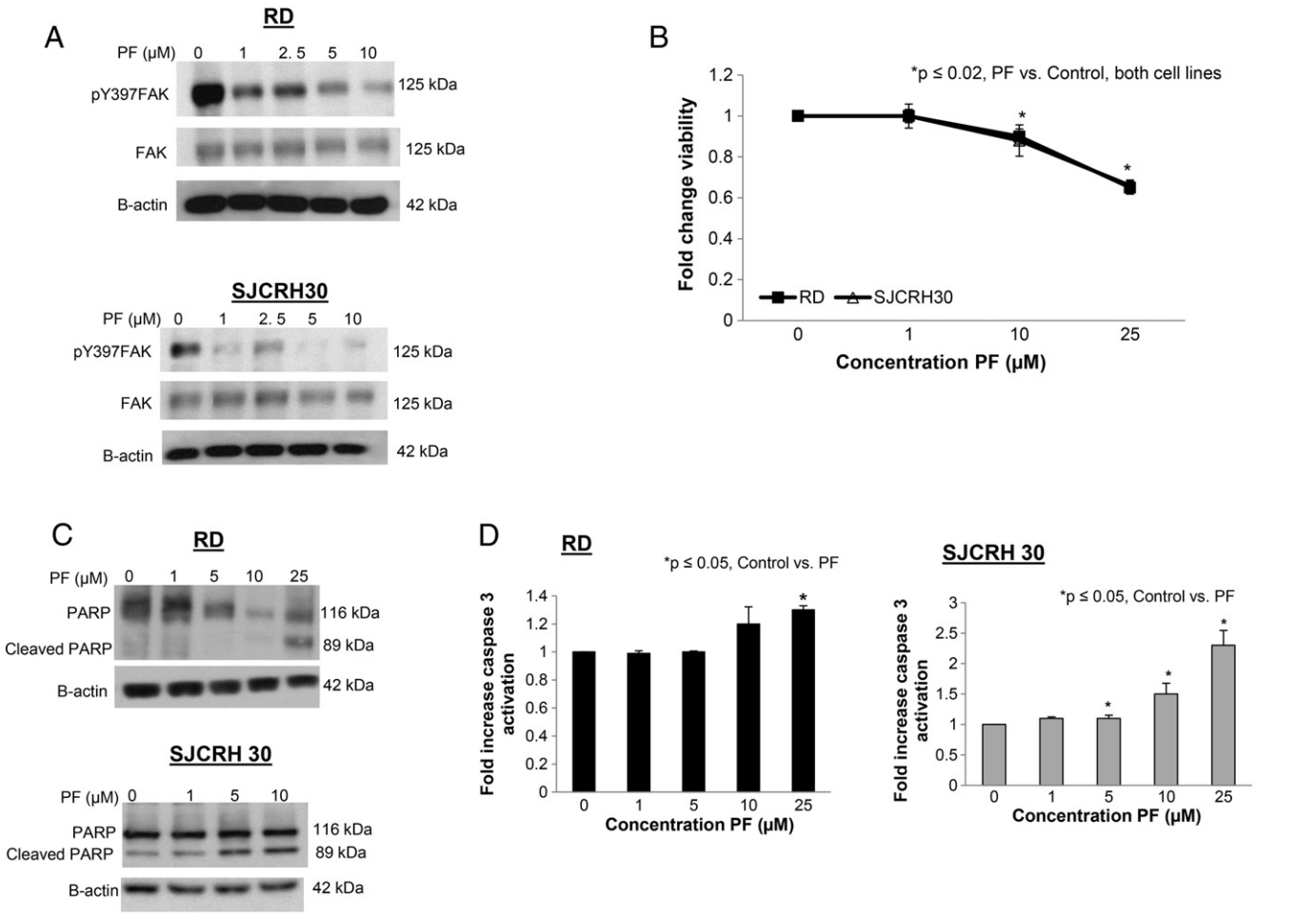

Figure 3. PF-573,228 (PF) inhibition of pY397FAK in human RMS cell lines. (A) RD and SJCRH30 cell lines were treated for 48 hours with increasing concentrations of PF. Cell lysates were harvested and evaluated with immunoblotting for total FAK and pY397FAK. Increasing concentrations of PF led to decreased pY397FAK in both cell lines. (B) AlamarBlue assays were used to assess cell viability. Both RD and SJCRH30 cell lines showed significantly decreased cell viability following treatment with PF for 48 hours. (C) Immunoblotting for cleaved PARP was utilized to detect apoptosis. RD and SJCRH30 cell lines were treated with PF for 48 hours, and cell lysates were collected. Immunoblotting showed increased cleaved PARP following PF treatment in both cell lines, indicating apoptosis. (D) RD and SJCRH30 cell lines were treated with PF at increasing concentrations for 48 hours, and caspase 3 activation was measured with a detection kit to document apoptosis. Significant increases in activated caspase 3 were detected in both cell lines. Data were from three independent experiments and reported as mean fold change ± SEM.

expression than the control tumors (Figure 7*C*). Densitometry was used to compare immunoblots from xenograft specimens, confirming decreased FAK expression after Y15 treatment (Figure 7*C*). Cell proliferation was measured in the tumor xenografts with immunohistochemistry staining for Ki67. The percentage of Ki67-positive cells was significantly decreased in the tumors treated with Y15 (49 ± 6% vs 64 ± 6%, Y15 vs control, $P = .03$). Representative photomicrographs (20×) are presented in Supplemental Data Figure S2, with negative controls reacting appropriately (Supplemental Data Figure S2, *small insert, left panel*).

SJCRH30 human ARMS cells (2.0×10^6) were injected into the right flank of 6-week-old female athymic nude mice ($n = 25$). Tumors were measured every 2 days, and tumor volumes were calculated as above. When tumors reached 200 mm^3, animals were randomized to receive intraperitoneal injections with either control (saline, $n = 10$) or Y15 ($n = 15$) for 2 weeks. Animals treated with Y15 had significantly less tumor growth than control-treated animals (Figure 7, *D* and *E*). The tripling time of the vehicle-treated tumors was significantly shorter than that of the Y15-treated animals (4.4 ± 1.0 days vs 9.9 ± 1.8 days, $P \le .02$, vehicle vs Y15). Knockdown of the target protein, FAK, was demonstrated by immunoblotting, showing that tumors treated with Y15 had less FAK protein than controls (Figure 7*F*). Densitometry was used to compare immunoblots from xenograft specimens, confirming decreased FAK expression after Y15 treatment (Figure 7*F*). The effect of Y15 upon tumor cell proliferation was evaluated with immunohistochemistry for Ki67. Tumors treated with Y15 had significantly less Ki67-positive cells than control-treated tumors (12 ± 6% vs 25 ± 4%, Y15 vs control, $P = .05$). Representative photomicrographs are displayed in Supplemental Data Figure S3. Negative control staining reacted appropriately (Supplemental Data Figure S3, *bottom insert, left panel*).

Discussion

RMS continues to pose a therapeutic challenge, highlighting the need for novel therapies. In this study, we explored the role of FAK in the tumorigenesis of two histologic and genetic subtypes of RMS:

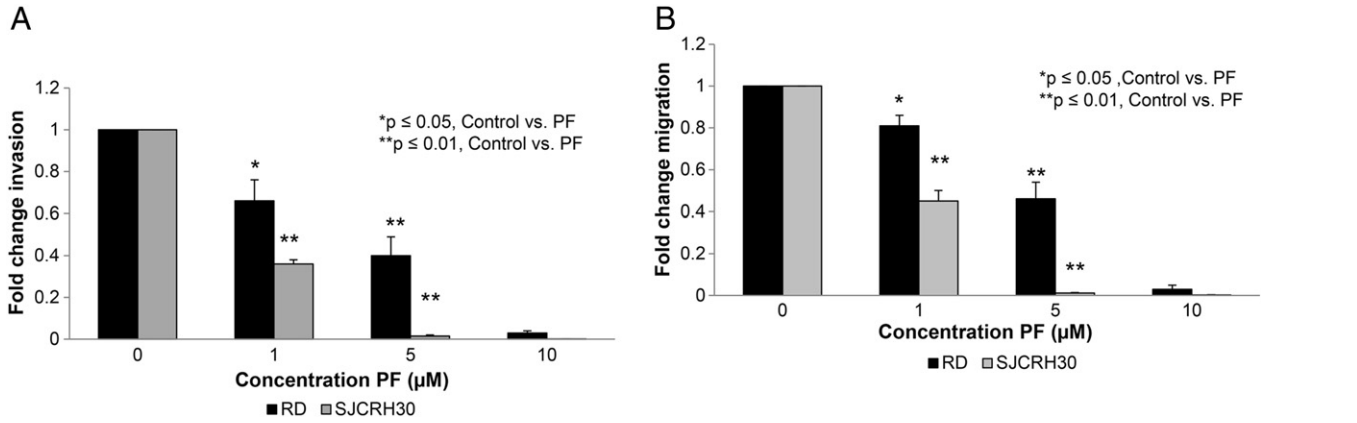

Figure 4. PF-573,228 (PF) treatment reduced invasion and migration of RMS cell lines. (A) RD and SJCRH30 cell lines were treated with PF at increasing concentrations and allowed to invade into a Matrigel-coated micropore insert for 48 hours. Invasion was reported as fold change in the number of cells invading. PF treatment resulted in a significant decrease in invasion in both cell lines at low concentrations of PF. (B) RD and SJCRH30 cell lines were treated with increasing concentrations of PF and allowed to migrate through a micropore insert for 24 hours. Migration was reported as fold change in the number of cells migrating through the membrane. Migration was significantly diminished following treatment with PF at a concentration of 1 μM. Data were from three independent experiments and reported as mean fold change ± SEM.

SJCRH30—alveolar (ARMS), *PAX3-FOXO1* fusion positive and RD—embryonal (ERMS), fusion negative. The rationale for the study of FAK in RMS was based upon the previous observations that kinases upstream or downstream from FAK have been identified as having a significant impact upon the tumorigenicity of RMS. For instance, inhibition of the upstream kinas, Src has been noted to decrease RMS cell growth both *in vitro* and *in vivo*[22]. Inhibition of Akt, a kinase downstream to FAK, has also been shown to inhibit RMS growth [23,24]. In addition, FAK was reported to be present in HT-1080 cells, a fibrosarcoma cell line [17]. These previous studies prompted us to hypothesize that FAK would be important in RMS and supported the need to describe its role in these tumors.

In the current investigations, we reported that FAK was expressed in human RMS tumor specimens, both ARMS and ERMS subtypes. To our knowledge, these findings are novel and have not been previously reported in the literature. Finding total and phosphorylated FAK in both subtypes has important clinical implications in that it implies that potential therapeutic interventions utilizing FAK inhibition would not be limited to a single subtype of RMS. Although both pY397FAK and FAK were detected in both ARMS and ERMS, there were factors precluding its use as a prognostic indicator. Because FAK and pY397FAK have been shown to be expressed in normal skeletal muscle [25,26], there was no opportunity to utilize normal tissue to assist in quantitating staining. Additionally, there was not enough of a difference in staining among the specimens, with almost all of them showing mild to moderate staining, and perhaps the limited number of specimens inhibited detection of small differences. Evaluations of Ewing sarcoma specimens have shown similar results [19,27] in that staining for FAK did not predict patient outcomes. Ren et al. did find that, in osteosarcoma, the presence of FAK protein and phosphorylation in human specimens correlated with both worse overall survival and worse metastasis-free survival [28]. Clearly, FAK may play an important role in multiple types of sarcomas, and perhaps FAK overexpression is a universal phenomenon not only for sarcomas but also for multiple solid tumors because it has been shown to be overexpressed in breast, colon, thyroid, head and neck, prostate, and ovarian cancers [29–33].

It was noted that the baseline FAK expression in the SJCRH30 cell line was less than that in the RD cell line, although the FAK phosphorylation was greater in the SJCRH30 cells. These findings may explain the observation that the SJCRH30 cell line was more sensitive to PF-induced inhibition of FAK phosphorylation, but these cells were also, in many regards, more sensitive to overall inhibition of FAK protein as seen with Y15 inhibitor. Obviously, it would follow that if the total protein were decreased, the amount of phosphorylated protein would also be decreased, leading to this finding. These findings could also be explained by the idea of oncogene addiction. Investigators have postulated that certain tumor cell lines are physiologically more dependent upon specific survival factors, and inhibition of these specific cellular factors will have a more profound effect upon those cells than others even of the same tumor type [34], regardless of their degree of expression. Another explanation is that there may be significant differences between cell lines that have the signature *PAX-FOXO1* fusion (SJCRH30) [18] and those that do not (RD), which would actually be an important finding because those tumors are the most aggressive and difficult to treat. Investigations into this hypothesis will certainly be the subject of future studies.

We found varying extents of change in PARP and caspase 3 depending upon the cell line and the agent utilized for FAK inhibition. These findings are likely due to differences in cell lines. Storch and colleagues had similar results when they examined PARP and caspase 3 in glioblastoma cell lines treated with FAK inhibition [35]. Four different ovarian cancer cell lines also had varying levels of PARP cleavage and caspase 3 activation with FAK inhibition [36].

The small molecule FAK inhibitor PF-573,228 was utilized in these studies to corroborate the siRNA findings that FAK was an important survival signal and a potential target in RMS tumors. PF-573,228 has been shown to block the FAK catalytic activity by binding to the ATP pocket of FAK [20]; decreasing cell survival, migration, and invasion [12,19]; as well as diminishing metastatic potential [37] and enhancing chemotherapy-induced cytotoxicity [38]. In an effort to minimize off-target effects associated with small molecule inhibitors, PF-573,228 was chosen over another FAK inhibitor, PF-562,271, because PF-562,271 affects PyK2 in addition

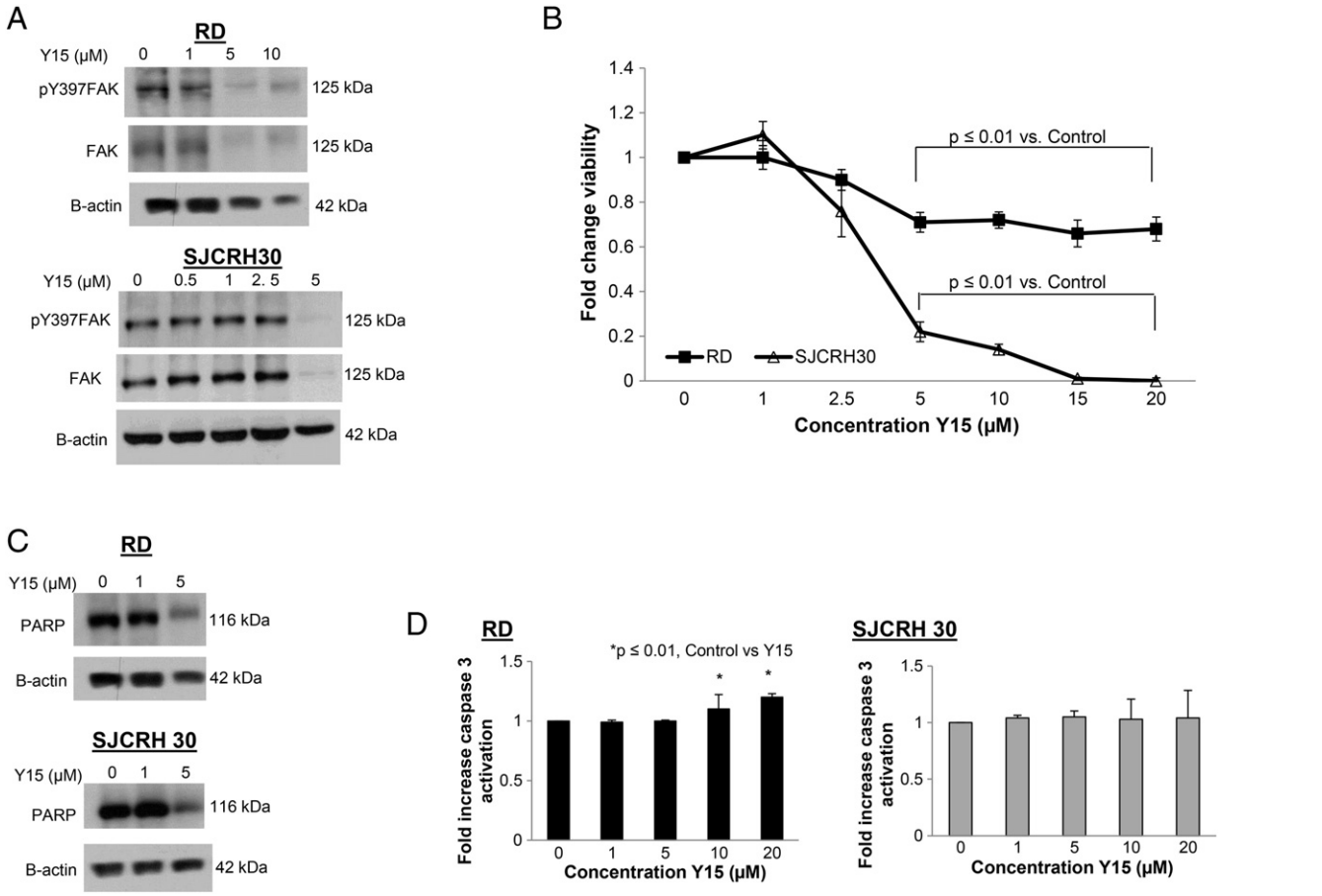

Figure 5. 1,2,4,5-Benzenetetraamine tetrahydrochloride (Y15) inhibition of FAK in human RMS cell lines. (A) RD and SJCRH30 cells were treated with increasing concentrations of Y15 for 24 hours, and lysates were collected. Immunoblotting showed decreased FAK expression in both cell lines. FAK phosphorylation followed total FAK expression. (B) AlamarBlue assay was used to measure cell viability. RD and SJCRH30 cells were treated with Y15 at increasing concentrations for 24 hours. Cell viability was significantly decreased with treatment of 5-μM concentration in both cell lines. (C) Immunoblotting was utilized to detect apoptosis. There was a decrease in total PARP detected in cell lysates from the RD and SJCRH30 cell lines after treatment with Y15, indicating apoptosis. (D) Apoptosis was also detected using a caspase 3 activation kit. Y15 resulted in a significant increase in caspase 3 activation in the RD cell line. Data were from three independent experiments and reported as mean fold change ± SEM.

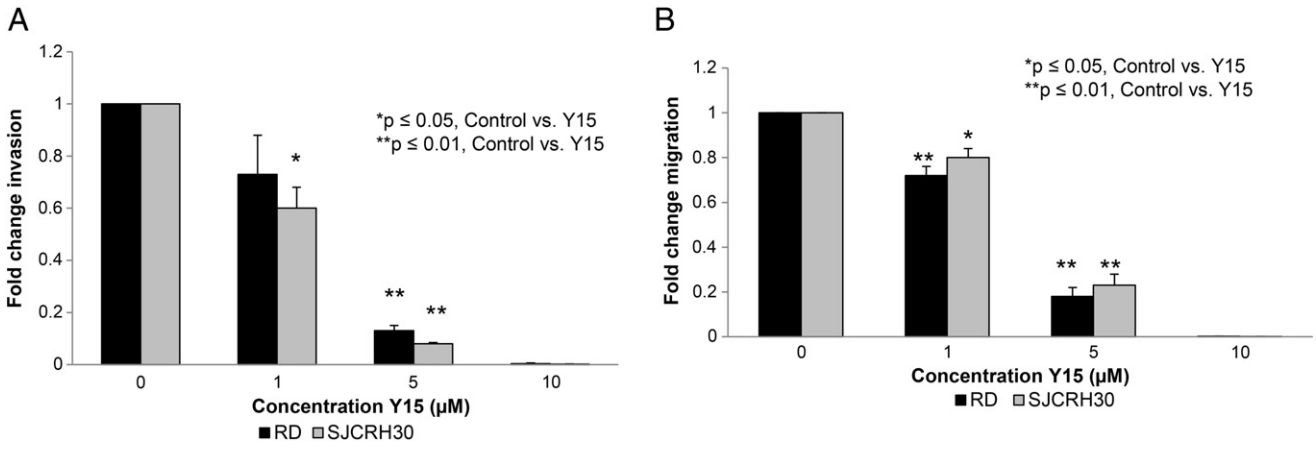

Figure 6. 1,2,4,5-Benzenetetraamine tetrahydrochloride (Y15) decreased cell invasion and migration. (A) RD and SJCRH30 cells were treated with increasing concentrations of Y15 and allowed to invade through a Matrigel-coated micropore insert. Invasion was reported as fold change in number of cells invading. Invasion was significantly decreased in both cell lines with increasing concentrations of Y15. (B). RD and SJCRH30 cells were treated with increasing concentrations of Y15 for 24 hours and allowed to migrate through a micropore insert. Migration was reported as fold change in number of cells migrating through the membrane. Migration was significantly decreased in both RMS cell lines with Y15 treatment, beginning at 1.0-μM concentration. Data were from three independent experiments and reported as mean fold change ± SEM.

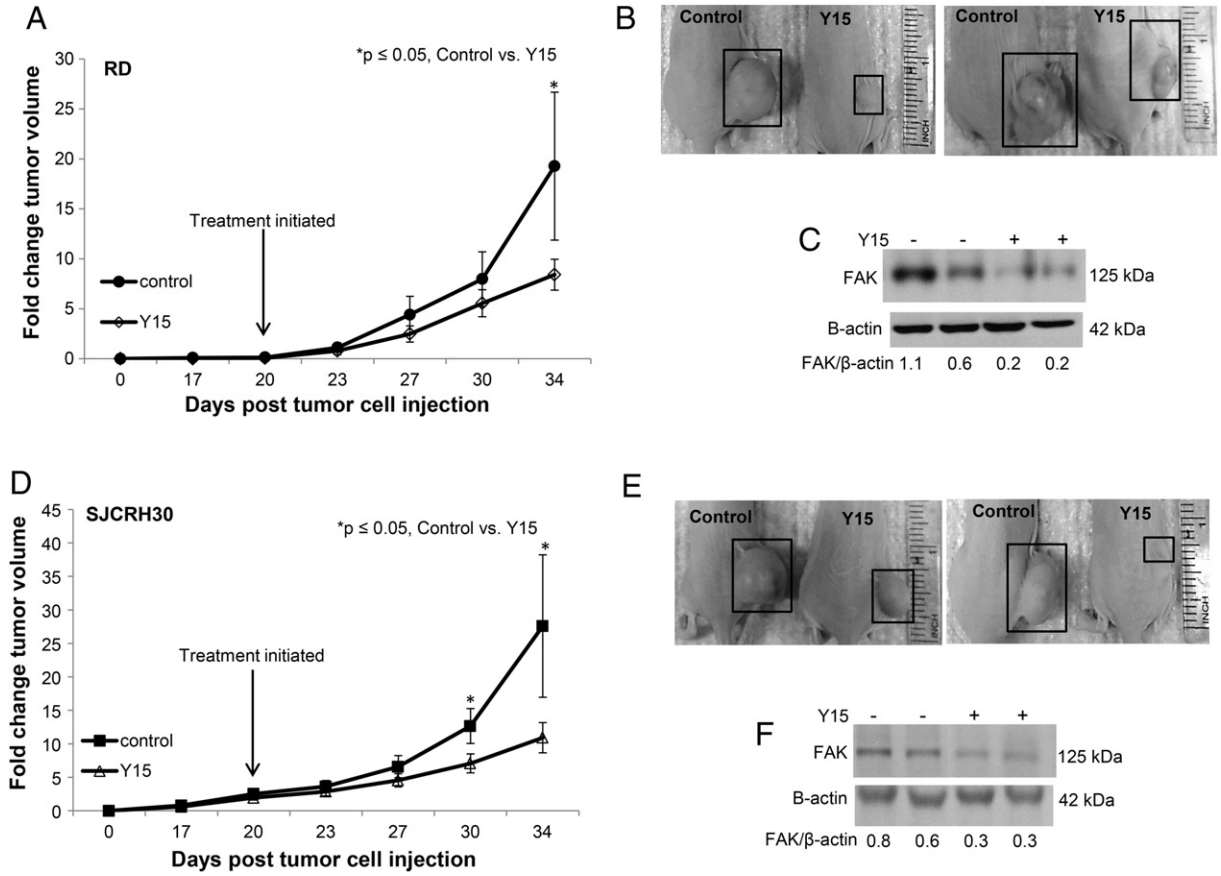

Figure 7. Treatment with 1,2,4,5-benzenetetraamine tetrahydrochloride (Y15) inhibited growth of human RMS xenografts. (A) RD embryonal RMS cells (2.5×10^6 cells/100 μl of sterile PBS) were injected into the subcutaneous space of the right flank of female nude mice ($n = 25$). When tumors reached 200 mm^3, the animals were randomized to daily intraperitoneal injection of control vehicle ($n = 10$) or Y15 ($n = 15$). Tumor volumes were measured and reported as fold change in tumor volume. Animals treated with Y15 had significantly less change in tumor volume compared with control-treated animals. (B) Representative photographs demonstrating differences in tumors between control and Y15-treated animals. (C) To confirm target knockdown in the RD specimens, immunoblotting for FAK was performed on xenograft tumor lysates. Tumors were homogenized, proteins wer separated on SDS-PAGE gels, and immunoblotting for FAK was performed, with representative immunoblots shown. There was a decrease in FAK in the tumors from the animals that received Y15 treatment. These findings were further demonstrated by densitometry, with a decreased FAK:β-actin ratio. (D) SJCRH30 RMS cells (2.0×10^6 cells/100 μl of sterile PBS) were injected into the subcutaneous space of the right flank of female nude mice ($n = 25$). When tumors reached 200 mm^3, animals were randomized to daily intraperitoneal injection of control vehicle ($n = 10$) or Y15 ($n = 15$). Tumor volumes were measured and reported as fold change in tumor volume. Animals treated with Y15 had significantly smaller change in tumor volume compared with controls. (E) Representative photographs demonstrating differences in tumors between animals treated with Y15 and controls. (F) To confirm target knockdown in the SJCRH30 specimens, immunoblotting for FAK was performed on xenograft tumor lysates. Representative immunoblots are shown. There was a decrease in FAK in the tumors from the animals that received Y15 treatment. These findings were further demonstrated by densitometry, showing a decreased FAK:β-actin ratio.

to FAK [39] and PF-573-228 does not [20]. However, PF-573,228 was not suitable for use *in vivo*; therefore, Y15 was utilized. Y15 has been previously described for *in vivo* use in a number of tumor models [14,16,19,40].

The metastatic potential of RMS cell lines appeared to be decreased as noted by decreased migration and invasion of the tumor cells following PF or Y15 treatment. The ability to metastases in a preclinical mouse model of RMS is currently difficult [41]. Subcutaneous injections of these cell lines do not routinely result in metastases that compare to the human condition. Tail vein injections of RMS result in intraperitoneal implants of tumor, but again, these conditions are far removed from those noted clinically in humans. Therefore, we were not able to explore this aspect of FAK inhibition in the current studies.

The small molecules PF-573,228 and Y15 have been reported to inhibit FAK phosphorylation at the Y397 autophosphorylation site [14,20]. In our study, we did see inhibition of pY397FAK in both cell lines with the PF-573-228, but the Y15 primarily affected total FAK expression and thereby subsequent FAK phosphorylation. Similar findings have been reported with other cell lines. Y15 treatment of the human pancreatic cell line Panc 1 decreased total FAK [15]; Y15 also resulted in decreased total FAK in studies with BT474 breast cancer cells [14] and U87 glioma cells [42].

In summary, we showed that multiple approaches to FAK abrogation including siRNA and small molecules diminished the malignant phenotype of RMS cell lines. There were a significant decrease in cell survival, an increase in apoptosis, and a decrease in both migration and invasion. An important observation was that the

changes in migration and invasion following small molecule FAK inhibition occurred at concentrations below the LD_{50} of the inhibitors because cells that are not viable will not invade or migrate. Another novel aspect of the current studies was the demonstration that FAK inhibition in a nude mouse model of RMS resulted in significantly smaller and less proliferative tumors when compared with controls. We believe that the data presented provide justification for further investigations of FAK inhibition as a potential therapeutic strategy for difficult-to-treat RMS.

Supplementary data to this article can be found online at http://dx.doi.org/10.1016/j.tranon.2016.06.001.

Acknowledgement

The work presented was funded in part by a grant from the National Cancer Institute (T32CA091078) (A.M.W., L.L.S., and E.F.G.). The content of this manuscript was solely the responsibility of the authors and does not necessarily represent the official views of the National Cancer Institute.

References

[1] Arndt CA and Crist WM (1999). Common musculoskeletal tumors of childhood and adolescence. *N Engl J Med* **341**, 342–352.

[2] Sultan I, Qaddoumi I, Yaser S, Rodriguez-Galindo C, and Ferrari A (2009). Comparing adult and pediatric rhabdomyosarcoma in the surveillance, epidemiology and end results program, 1973 to 2005: an analysis of 2,600 patients. *J Clin Oncol* **27**, 3391–3397.

[3] Sorensen PH, Lynch JC, Qualman SJ, Tirabosco R, Lim JF, Maurer HM, Bridge JA, Crist WM, TRiche TH, and Barr FG (2002). PAX3-FKHR and PAX7-FKHR gene fusions are prognostic indicators in alveolar rhabdomyosarcoma: a report from the children's oncology group. *J Clin Oncol* **20**, 2672–2679.

[4] Oberlin O, Rey A, Lyden E, Bisogno G, Stevens MC, Meyer WH, Carli M, and Anderson JR (2008). Prognostic factors in metastatic rhabdomyosarcomas: results of a pooled analysis from United States and European cooperative groups. *J Clin Oncol* **26**, 2384–2389.

[5] Xing Z, Chen HC, Nowlen JK, Taylor SJ, Shalloway D, and Guan JL (1994). Direct interaction of v-Src with the focal adhesion kinase mediated by the Src SH2 domain. *Mol Biol Cell* **5**, 413–421.

[6] Schaller MD, Borgman CA, Cobb BS, Vines RR, Reynolds AB, and Parsons JT (1992). pp125FAK a structurally distinctive protein-tyrosine kinase associated with focal adhesions. *Proc Natl Acad Sci U S A* **89**, 5192–5196.

[7] Hanks SK and Polte TR (1997). Signaling through focal adhesion kinase. *BioEssays* **19**, 137–145.

[8] Gabarra-Niecko V, Schaller MD, and Dunty JM (2003). FAK regulates biological processes important for the pathogenesis of cancer. *Cancer Metastasis Rev* **22**, 359–374.

[9] Chen HC and Guan JL (1994). Association of focal adhesion kinase with its potential substrate phosphatidylinositol 3-kinase. *Proc Natl Acad Sci U S A* **91**, 10148–10152.

[10] Schlaepfer DD, Hauck CR, and Sieg DJ (1999). Signaling through focal adhesion kinase. *Prog Biophys Mol Biol* **71**, 435–478.

[11] Han EK, Mcgonigal T, Wang J, Giranda VL, and Luo Y (2004). Functional analysis of focal adhesion kinase (FAK) reduction by small inhibitory RNAs. *Anticancer Res* **24**, 3899–3905.

[12] Megison ML, Stewart JE, Nabers HC, Gillory LA, and Beierle EA (2012). FAK inhibition decreases cell invasion, migration and metastasis in MYCN amplified neuroblastoma. *Clin Exp Metastasis* **30**, 555–568.

[13] Beierle EA, Ma X, Trujillo A, Kurenova EV, Cance WG, and Golubovskaya VM (2010). Inhibition of focal adhesion kinase and src increases detachment and apoptosis in human neuroblastoma cell lines. *Mol Carcinog* **49**, 224–234.

[14] Golubovskaya VM, Nyberg C, Zheng M, Kweh F, Magis A, Ostrov D, and Cance WG (2008). A small molecule inhibitor, 1,2,4,5-benzenetetraamine tetrahydrochloride, targeting the y397 site of focal adhesion kinase decreases tumor growth. *J Med Chem* **51**, 7405–7416.

[15] Hochwald SN, Nyberg C, Zheng M, Zheng D, Wood C, Massoll NA, Magis A, Ostrov D, Cance WG, and Golubovskaya VM (2009). A novel small molecule inhibitor of FAK decreases growth of human pancreatic cancer. *Cell Cycle* **8**, 2435–2443.

[16] Beierle EA, Ma X, Stewart J, Nyberg C, Trujillo A, Cance WG, and Golubovskaya VM (2010). Inhibition of focal adhesion kinase decreases tumor growth in human neuroblastoma. *Cell Cycle* **9**, 1005–1015.

[17] Perry BC, Wang S, and Basson MD (2010). Extracellular pressure stimulates adhesion of sarcoma cells via activation of focal adhesion kinase and Akt. *Am J Surg* **200**, 610–614.

[18] Fredericks WJ, Galili N, Mukhopadhyay S, Rovera G, Bennicelli J, Barr FG, and Rauscher FJ (1995). The PAX3-FKHR fusion protein created by the t(2;13) translocation in alveolar rhabdomyosarcomas is a more potent transcriptional activator than PAX3. *Mol Cell Biol* **15**, 1522–1535.

[19] Megison ML, Gillory LA, Stewart JE, Nabers HC, Mroczek-Musulman E, and Beierle EA (2014). FAK inhibition abrogates the malignant phenotype in aggressive pediatric renal tumors. *Mol Cancer Res* **12**, 514–526.

[20] Slack-Davis JK, Martin KH, Tilghman RW, Iwanicki M, Ung EJ, Autry C, Luzzio MJ, Cooper B, Kath JC, and Roberts WG, et al (2007). Cellular characterization of a novel focal adhesion kinase inhibitor. *J Biol Chem* **282**, 14845–14852.

[21] Hauck CR, Sieg DJ, Hsia DA, Loftus JC, Gaarde WA, Monia BP, and Schlaepfer DD (2001). Inhibition of focal adhesion kinase expression or activity disrupts epidermal growth factor-stimulated signaling promoting the migration of invasive human carcinoma cells. *Cancer Res* **61**, 7079–7090.

[22] Casini N, Forte IM, Mastrogiovanni G, Pentimalli F, Angelucci A, Festuccia C, Tomei V, Ceccherini E, Di Marzo D, and Schenone S, et al (2015). SRC family kinase (SFK) inhibition reduces rhabdomyosarcoma cell growth in vitro and in vivo and triggers p38 MAP kinase-mediated differentiation. *Oncotarget* **6**, 12421–12435.

[23] Srivastava RK, Kaylani SZ, Edrees N, Li C, Talwelkar SS, Xu J, Palle K, Pressey JG, and Athar M (2014). GLI inhibitor GANT-61 diminishes embryonal and alveolar rhabdomyosarcoma growth by inhibiting Shh/AKT-mTOR axis. *Oncotarget* **5**, 12151–12165.

[24] Graab U, Hahn H, and Fulda S (2015). Identification of a novel synthetic lethality of combined inhibition of hedgehog and PI3K signaling in rhabdomyosarcoma. *Oncotarget* **6**, 8722–8735.

[25] Bae GU, Yang YJ, Jiang G, Hong M, Lee HJ, Tessier-Lavigne M, Kang JS, and Krauss RS (2009). Neogenin regulates skeletal myofiber size and focal adhesion kinase and extracellular signal-regulated kinase activities in vivo and in vitro. *Mol Biol Cell* **20**, 4920–4931.

[26] Sakuma K, Nakao R, Inashima S, Hirata M, Kubo T, and Yasuhara M (2004). Marked reduction of focal adhesion kinase, serum response factor and myocyte enhancer factor 2C, but increase in RhoA and myostatin in the hindlimb dy mouse muscles. *Acta Neuropathol* **108**, 241–249.

[27] Crompton BD, Carlton AL, Thorner AR, Christie AL, Du J, Calicchio ML, Rivera MN, Fleming MD, Kohl NE, and Kung AL, et al (2013). High-throughput tyrosine kinase activity profiling identifies FAK as a candidate therapeutic target in Ewing sarcoma. *Cancer Res* **73**, 2873–2883.

[28] Ren K, Lu X, Yao N, Chen Y, Yang A, Chen H, Zhang J, Wu S, Shi X, and Wang C, et al (2015). Focal adhesion kinase overexpression and its impact on human osteosarcoma. *Oncotarget* **6**, 31085–31103.

[29] Cance WG, Harris JE, Iacocca MV, Roche E, Yang X, Chang J, Simkins S, and Xu L (2000). Immunohistochemical analyses of focal adhesion kinase expression in benign and malignant human breast and colon tissues: correlation with preinvasive and invasive phenotypes. *Clin Cancer Res* **6**, 2417–2423.

[30] Owens LV, Xu L, Dent GA, Yang X, Sturge GC, Craven RJ, and Cance WG (1996). Focal adhesion kinase as a marker of invasive potential in differentiated human thyroid cancer. *Ann Surg Oncol* **3**, 100–105.

[31] Kornberg LJ (1998). Focal adhesion kinase expression in oral cancers. *Head Neck* **20**, 634–639.

[32] Slack JK, Adams RB, Rovin JD, Bissonette EA, Stoker CE, and Parsons JT (2001). Alterations in the focal adhesion kinase/Src signal transduction pathway correlate with increased migratory capacity of prostate carcinoma cells. *Oncogene* **20**, 1152–1163.

[33] Judson PL, He X, Cance WG, and Van Le L (1999). Overexpression of focal adhesion kinase, a protein tyrosine kinase, in ovarian carcinoma. *Cancer* **86**, 1551–1556.

[34] Weinstein IB (2002). Cancer. Addiction to oncogenes — the Achilles heal of cancer. *Science* **297**, 63–64.

[35] Storch K, Sagerer A, and Cordes N (2009). Cytotoxic and radiosensitizing effects of FAK targeting in human glioblastoma cells in vitro. *Oncol Rep* **33**, 2009–2016.

[36] Yoon H, Choi YL, Song JY, Do I, Kang SY, Ko YH, Song S, and Kim BG (2014). Targeted inhibition of FAK, PYK2 and BCL-XL synergistically enhances apoptosis in ovarian clear cell carcinoma cell lines. *PLoS One* **9**e88587.

[37] Wendt MK and Schiemann WP (2009). Therapeutic targeting of the focal adhesion complex prevents oncogenic TGF-beta signaling and metastasis. *Breast Cancer Res* **11**, R68.

[38] Huanwen W, Zhiyong L, Xiaohua S, Xinyu R, Kai W, and Tonghua L (2009). Intrinsic chemoresistance to gemcitabine is associated with constitutive and laminin-induced phosphorylation of FAK in pancreatic cancer cell lines. *Mol Cancer* **8**, 125.

[39] Ocak S, Yamashita H, Udyavar AR, Miller AN, Gonzalez AL, Zou Y, Jiang A, Yi Y, Shyr Y, and Estrada L, et al (2010). DNA copy number aberrations in small-cell lung cancer reveal activation of the focal adhesion pathway. *Oncogene* **29**, 6331–6342.

[40] Lee S, Qiao J, Paul P, O'Connor KL, Evers MB, and Chung DH (2012). FAK is a critical regulator of neuroblastoma liver metastasis. *Oncotarget* **3**, 1576–1587.

[41] Norris RE and Adamson PC (2012). Challenges and opportunities in childhood cancer drug development. *Nat Rev Cancer* **12**, 776–782.

[42] Golubovskaya VM, Huang G, Ho B, Yemma M, Morrison CD, Lee J, Eliceiri BP, and Cance WG (2013). Pharmacologic blockade of FAK autophosphorylation decreases human glioblastoma tumor growth and synergizes with temozolomide. *Mol Cancer Ther* **12**, 162–172.